Integrated Transmission Systems Convex Optimal Power Flow Considering Security Constraints

Biswajit Dipan Biswas$^{\oplus}$, Seyedmahdi Moghadasi$^{\oplus}$, Sukumar Kamalasadan$^{\oplus}$, and Sumit Paudyal$^{\diamond}$
$^{\oplus}$ University of North Carolina, Charlotte; $^{\diamond}$Michigan Technological University, USA
Emails: bbiswas@uncc.edu, smoghada@uncc.edu, skamalas@uncc.edu, sumitp@mtu.edu

***Abstract*—In this paper, a new voltage stability constrained optimal power flow (VSC-OPF) model is developed using semi-definite programming (SDP), which optimally calculates the loading and the cost of increasing stability margins. The main advantages of the proposed method are: a) incorporates voltage stability constraints in a convex OPF formulation b) always finds the optimal solution in comparison with probable local optimum solutions while using other non-convex methods, and c) can compare the cost of increasing the loading margin using convex relaxation. The effectiveness of this method is evaluated using the IEEE 14-bus and 118-bus test systems with various network constraints. The results show that the proposed convex formulation find the optimal operating schedule and critical loading point. The effect of incorporating voltage stability margin can also be examined using the proposed method.**

***Index Terms*—OPF, Transmission System, Convex Optimization, Voltage Stability, Semi-Definite Programming (SDP).**

I. Nomenclature

i, j	bus index
N_G	set of generation buses
x	state variables in OPF
P, Q, S	active, reactive and apparent power
$g(.), h(.)$	equality and inequality constraints of OPF
$f(.)$	current and maximum loading point function
λ,λ^m	current and maximum loading points
ω_1, ω_2	coefficients of cost and loading margin
v_i, δ_i	voltage magnitude and voltage angle of bus i
W,W^m	$2n \times 2n$ positive semidefinite matrices
c_i, C_{i_k}	cost function and cost coefficient at bus i
$\bar{\delta}_{max}$	maximum angle deviation
$\triangle\lambda_{min}$	minimum loading distance
P_{D_i},Q_{D_i}	active and reactive load connected at bus i
Y_i, Y_{ij}	System admittance matrices
J_i^k	Coefficient matrices
K_{ij}^k, L_{ij}	Coefficient matrices for angle relaxation
Tr	Matrix trace
a_i, a_i^m, $\bar{a}_i$, $\bar{a}_i^m$	min & max limits of dependent & independent variables

This work was supported in part by the NSF grant ECCS-1810174 awarded to the third author, and in part by the NSF grant ECCS-1751460 awarded to the fourth author.

II. Introduction

In the age of large, renewable energy integrated dynamic power system, the transmission systems are changing frequently with added generations and demands. This radical changes poses a severe stress on system stability. As a result, there is a need of fast optimal power flow (OPF) method to calculate the dispatches for the generation resources [1]. Various methods have been introduced to solve the OPF problem since 1930's when it started basically for economic dispatch [2]. OPF problem is non-convex because of the non-linear power flow equations. The OPF problem is also NP hard [3], because of which it is difficult to reach an exact global solution. Main methods that have been studied include Linear Programming, Non-linear Programming, Quadratic Programming, Interior point methods, and methods using Artificial Intelligence [4]. Dynamic and heavily stressed modern power grid because of high power utilization by the consumer and large changing generation source needs a special attention on system voltage stability for solving OPF. Thus, optimal power flow methods are formulated having voltage stability as a constraint in problem formulation or using the objective function for stability margin [5]. Some of the earlier methods reported in the literature introduces an index called voltage collapse proximity indicator and include it in the constraints or objective function [6], [7].

Wide range of study for finding more accurate and fast method for OPF has been reported in the literature [8]. Recently the research in the field of convexification of OPF problem is quite notable [9], [10]. One of the most popular methods is DC-OPF, where the power flow equations are linearized by imposing few approximations for voltage magnitudes, angles and line impedance. For radial system, second order conic programming (SOCP) in branch flow model is another effective method and for general system semi-definite programming (SDP) relaxation [11] using bus injection model is most accurate [12] [13]. In [14], the SDP relaxation is analyzed and used to formulate the dual of an equivalent of OPF problem. For the distribution networks, SOCP method is used to convexify the problem constraints which enables the controller to achieve global solution for a faster computation time [15]. This method is implemented on a more detailed system incorporating neighboring DISCO, distributed generators, wind generator and energy storage systems [16]. Ref. [17], [18] and [19] has discussed convexification methods of OPF problem for

transmission system using SDP relaxation by incorporating convexification and VSC-OPF. These studies analyze the methods on the basis of stability margin index or total operation cost.

In this paper a new convex method is proposed that focuses on the stability margin index as well as the node voltage angles to analyze the system stability and optimality. In the problem formulation, the voltage angles have been relaxed to convexify the constraints. Then after convergence, the angles are recovered implementing the angle recovery algorithm. Then analyzing the node voltage magnitudes, angles, and the total cost, the optimal solution is derived. The proposed method has the following advantages:

- The method is convex which overcome the local solution problem of the non-convex optimal power flow methods.
- Along with voltage magnitudes and total cost, voltage angles are also recovered to get the total overview of the power system.
- This method is scalable and works seemlessly for larger system with different types of generation resources.

The rest of the paper is organised in the following pattern. In section III, general formulation of the proposed method described. It includes formulation of VSC-OPF in III-A, convexification algorithm in III-B and the angle recovery method in III-C. Then, in section IV the proposed method has been implemented in IEEE 14 bus and 118 bus transmission systems and the results are discussed. Finally, conclusions and future work is included in section V.

III. Problem Formulation

A. Voltage Security Constraint OPF

The objective of voltage stability constrained OPF is to dispatch the optimal operating point and also at the same time maximize the stabily margin. The generalized VSC-OPF problem can be formulated as [20].

$$\text{Min} \sum_{i} z_i\left(x, \lambda, \lambda^m, \Gamma_i\right) \tag{1}$$

$$\text{s.t.} \begin{cases} h(x, \gamma_i, \lambda_i) = 0 \\ h(x^m, \gamma_i^m, \lambda_i^m) = 0 \\ \underline{a}_i \le g\left(x, \lambda, \gamma_i\right) \le \bar{a}_i \\ \underline{a}_i^m \le g\left(x^m, \lambda^m, \gamma_i^m\right) \le \bar{a}_i^m \\ \underline{b}_i \le f(\lambda, \lambda^m) \le \bar{b}_i \end{cases}$$

The functions h(.) and g(.) represents the equality and inequality constraints of the problem which are bounded by the lower and upper limits of the dependent and independent variables. Here, $x \in N$ denotes the dependent variable of the system which is the node voltage magnitude. Vector $\gamma \in N_G$ represents the set of independent variable of the system, which is active and reactive power generation at the generator buses. The λ and λ^m stands for the parameter loading factor. The proposed formulation includes both cost minimization and maximizing the voltage stability margin as the objective function. Two weighting factors ω_1 and ω_2 have been introduced to further optimize the contribution of each objective for the global solution. Based on this the objective function in (1) can be reformulated as follows

$$\begin{aligned} \text{Min} \;\; \omega_1 \sum_{i \in N_G} \{ & C_{i_2}\left(P_{G_i}\right)^2 \\ & + C_{i_1}\left(P_{G_i}\right) + C_{i_0}\} - \omega_2\left(\lambda^m - \lambda\right) \end{aligned} \tag{2}$$

where $\omega_1 + \omega_2 = 1$

B. Convexification Procedure

The convexification procedure of the VSC-OPF problem using the semi-definite programming is as follows. First, two vectors of voltages are considered; the current opreating voltage vector and maximum loading point of the system. The current operating point voltage vector is denoted as $V = \left[\text{Re}\{v\}^T \text{Im}\{v\}^T\right]$ and the maximum loading point voltage vector is denoted as $V^m = \left[\text{Re}\{v^m\}^T \text{Im}\{v^m\}^T\right]$. The variables λ and λ^m denote the current and maximum loading points with V and V^m in the VSC-OPF problem expressed as a quadratic equations. To transform the quadratic equation in to a linear equation, VV^T and $V^m V^{mT}$ are replaced by another matrices W and W^m respectively. Equation (3) represents the objective function and constraints and Equation (4) represents all the matrices that are used to convexify the VSC-OPF problem. The angle drop constraint of the node voltages is in the form shown in (5) which can be written as (6). Modification of (6) can be written using the real and imaginary part of voltage, which is shown in (7). Using the semi-definite programming, these equations can be expressed as convex constraints as shown in (8)-(10). All the required notations are given in Section I.

$$\begin{aligned} \text{Min} \;\; \omega_1 \sum_{i \in N_G} \{ & C_{i_2}\left(\text{Tr}\{Y_i W\} + \lambda P_{D_i}\right)^2 \\ & + C_{i_1}\left(\text{Tr}\{Y_i W\} + \lambda P_{D_i}\right) + C_{i_0}\} + \omega_2\left(\lambda^m - \lambda\right) \end{aligned} \tag{3}$$

$$\text{s.t.} \begin{cases} P_i^{min} \le \text{Tr}\{Y_i W\} + \lambda P_{D_i} \le P_i^{max} \\ P_i^{min} \le \text{Tr}\{Y_i W^m\} + \lambda^m P_{D_i} \le P_i^{max} \\ Q_i^{min} \le \text{Tr}\{\bar{Y}_i W\} + \lambda Q_{D_i} \le Q_i^{max} \\ Q_i^{min} \le \text{Tr}\{\bar{Y}_i W^m\} + \lambda^m Q_{D_i}^m \le Q_i^{max} \\ \left(V_i^{min}\right)^2 \le \text{Tr}\{J_i W\} \le \left(V_i^{max}\right)^2 \\ \left(V_i^{min}\right)^2 \le \text{Tr}\{J_i W^m\} \le \left(V_i^{max}\right)^2 \\ \text{Tr}\{Y_{ij} W\} \le P_{ij}^{max} \\ \text{Tr}\{Y_{ij} W^m\} \le P_{ij}^{max} \\ \text{Tr}\{J_{ij} W\} \le \triangle\left(V_{ij}\right)^2 \\ \text{Tr}\{J_{ij} W^m\} \le \triangle\left(V_{ij}\right)^2 \\ \omega_1 + \omega_2 = 1 \\ \alpha \times (\lambda^m - \lambda) \ge \triangle\lambda_{min} \\ \tan(\delta_{max}) \times \text{Tr}\{K_{ij} W\} - \text{Tr}\{L_{ij} W\} \ge 0 \\ \tan(\delta_{max}) \times \text{Tr}\{K_{ij} W^m\} - \text{Tr}\{L_{ij} W^m\} \ge 0 \\ W = VV^T \\ W^m = V^m V^{mT} \end{cases}$$

$$Y_{e_n} = e_n e_n^T; \quad Y_{e_{ij}} = \left(\bar{y}_{ij} + y_{ij}\right) e_i e_i^T - \left(y_{ij}\right) e_i e_j^T \tag{4}$$

$$Y_{1_n} = Y_{e_n} + Y_{e_n}^T; \quad Y_{2_n} = Y_{e_n} - Y_{e_n}^T$$

$$Y_{1_{ij}} = Y_{e_{ij}} + Y_{e_{ij}}^T; \quad Y_{2_{ij}} = Y_{e_{ij}} - Y_{e_{ij}}^T$$

$$Y_n = \frac{1}{2}\begin{bmatrix} \mathrm{Re}\left(Y_{1_n}\right) & -\mathrm{Im}\left(Y_{2_n}\right) \\ -\mathrm{Im}\left(Y_{2_n}\right) & \mathrm{Re}\left(Y_{1_n}\right) \end{bmatrix}$$

$$\bar{Y}_n = -\frac{1}{2}\begin{bmatrix} \mathrm{Im}\left(Y_{1_n}\right) & \mathrm{Re}\left(Y_{2_n}\right) \\ -\mathrm{Re}\left(Y_{2_n}\right) & \mathrm{Im}\left(Y_{1_n}\right) \end{bmatrix}$$

$$Y_{ij} = \frac{1}{2}\begin{bmatrix} \mathrm{Re}\left(Y_{1_{ij}}\right) & -\mathrm{Im}\left(Y_{2_{ij}}\right) \\ -\mathrm{Im}\left(Y_{2_{ij}}\right) & \mathrm{Re}\left(Y_{1_{ij}}\right) \end{bmatrix}$$

$$\bar{Y}_{ij} = -\frac{1}{2}\begin{bmatrix} \mathrm{Im}\left(Y_{1_{ij}}\right) & \mathrm{Re}\left(Y_{2_{ij}}\right) \\ -\mathrm{Re}\left(Y_{2_{ij}}\right) & \mathrm{Im}\left(Y_{1_{ij}}\right) \end{bmatrix}$$

$$J_n = \frac{1}{2}\begin{bmatrix} e_n e_n^T & 0 \\ 0 & e_n e_n^T \end{bmatrix}$$

$$J_{ij} = \frac{1}{2}\begin{bmatrix} \left(e_i - e_j\right)\left(e_i - e_j\right)^T & 0 \\ 0 & \left(e_i - e_j\right)\left(e_i - e_j\right)^T \end{bmatrix}$$

$$V = \begin{bmatrix} \mathrm{Re}\{v\}^T \mathrm{Im}\{v\}^T \end{bmatrix}$$

$$V^m = \begin{bmatrix} \mathrm{Re}\{v^m\}^T \mathrm{Im}\{v^m\}^T \end{bmatrix}$$

$$\delta_i - \delta_j \leq \delta_{max} \qquad \forall\,(i,i) \in N_L \tag{5}$$

$$\tan\left(\delta_i - \delta_j\right) \leq \tan\left(\delta_{max}\right) \qquad \forall\,(i,j) \in N_L \tag{6}$$

$$\tan\left(\delta_i - \delta_j\right) = \frac{\mathrm{Re}\{V_j\}\mathrm{Im}\{V_i\} - \mathrm{Re}\{V_i\}\mathrm{Im}\{V_j\}}{\mathrm{Re}\{V_i\}\mathrm{Re}\{V_j\} + \mathrm{Im}\{V_i\}\mathrm{Im}\{V_j\}} \tag{7}$$

$$\tan\left(\delta_{max}\right) \times \mathrm{Tr}\{K_{ij}W\} - \mathrm{Tr}\{L_{ij}W\} \geq 0 \tag{8}$$

$$L_{ij} = \frac{1}{2}\begin{bmatrix} 0 & e_i e_j^T - e_j e_i^T \\ e_i e_j^T - e_j e_i^T & 0 \end{bmatrix} \tag{9}$$

$$K_{ij} = \frac{1}{2}\begin{bmatrix} e_i e_j^T + e_j e_i^T & 0 \\ 0 & e_i e_j^T + e_j e_i^T \end{bmatrix} \tag{10}$$

C. Angle Recovery

In the SDP method the angle recovery after the optimal power flow is a major concern. In this proposed algorithm, using the optimized value of the Positive-Semi-Definite (PSD) matrix W, all other parameters are calculated. We can re-write the (9) as follows for angle recovery purpose.

$$\tan(\delta_{ij}) \geq \frac{\mathrm{Tr}\{L_{ij}W\}}{\mathrm{Tr}\{K_{ij}W\}} \tag{11}$$

From (11), the numerator and the denominator values are extracted from GAMS optimization package and then using MATLAB the node voltage angle differences are calculated. Further, considering the slack bus voltage angle same as the initial value, all other node voltage angles are calculated.

IV. Case Studies

The VSC-OPF methodology proposed in this paper was applied to two IEEE test systems. The first test system is the IEEE 14 bus system. It has 5 synchronous machines, 16 lines and 3 transformers. Bus 1 works as the slack bus which contains the largest generator as well. The cost coefficients of the generators are given in Table I. The second system, IEEE 118 bus system is considered to test the algorithm for a larger system. This system includes 19 generators, 35 synchronous condensers, 177 lines, 9 transformers and 91 loads. Here the slack bus is bus 69. Fig. 1 and fig. 2 reprsents the test systems. All the case studies are conducted using a PC equipped with 2.5GHz i7 processor and 8GB RAM. For the proposed methodology the GAMS optimization software with MOSEK solver package is used. Three cases are considered to evaluate the proposed method.

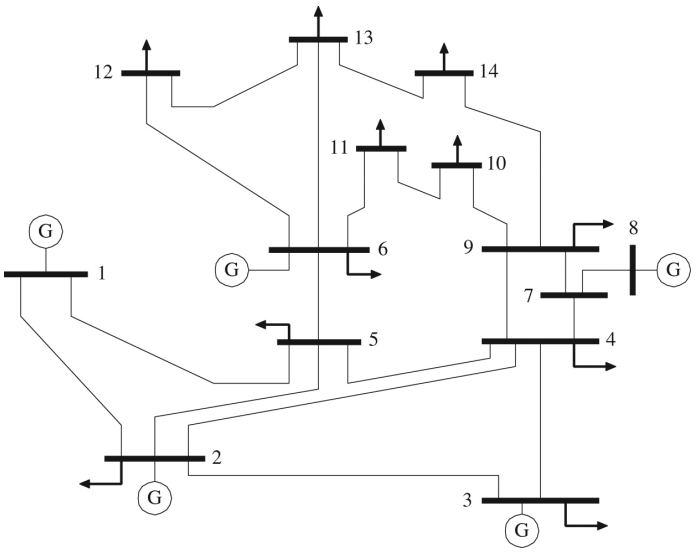

Fig. 1: IEEE 14 Bus Transmission Test System.

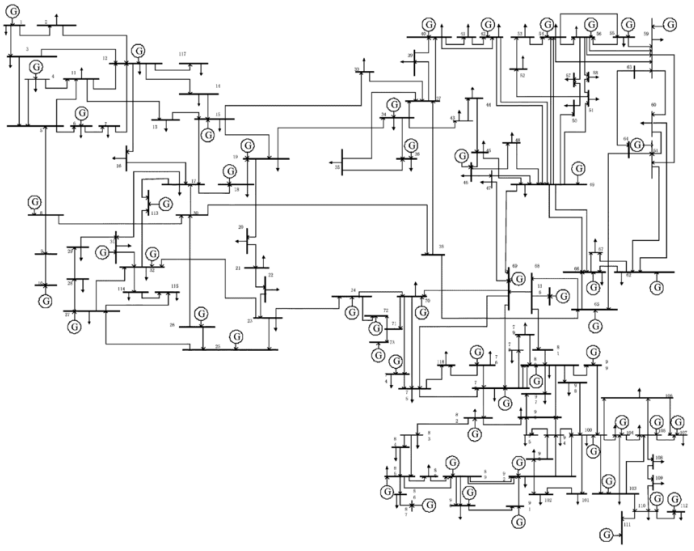

Fig. 2: IEEE 118 Bus Transmission Test System.

A. Case1

In this case [17] the objective function consists of cost minimization. So, the modified objective function is

$$\text{Min} \quad \sum_{i \in N_G} \{C_{i_2} \left(\text{Tr}\{Y_i W\} + \lambda P_{D_i}\right)^2 + C_{i_1} \left(\text{Tr}\{Y_i W\} + \lambda P_{D_i}\right) + C_{i_0}\} \tag{12}$$

The constraints remains the same as in (3).

B. Case2

In this case, the objective function emphasizes on maximizing the stability margin rather that cost or loss minimization. So, the objective function takes the form as,

$$\text{Min} \quad -\left(\lambda^m - \lambda\right) \tag{13}$$

C. Case3

In this case, both the cost minimization and loading stability margin maximization are combined as descried in (3).

In the results shown below, it is seen that, this proposed approach provides flexibility to the system operator to increase the loading of the system while keeping the generation cost at its minimum value.

Both the 14 bus system and 118 bus system have been simulated for all the three cases. Fig 3, 4 and Fig 5, 6 shows the node voltage magnitude and angle of IEEE 14 bus and 118 bus transmission system. It can be seen that, voltage magnitude for cost minimization is lower than the voltage stability maximization case, since the power generation is higher in the case 2. However, for the combined objective function, in case 3, the voltage magnitude is improved compared to case 1 and not as robust as in case 2.

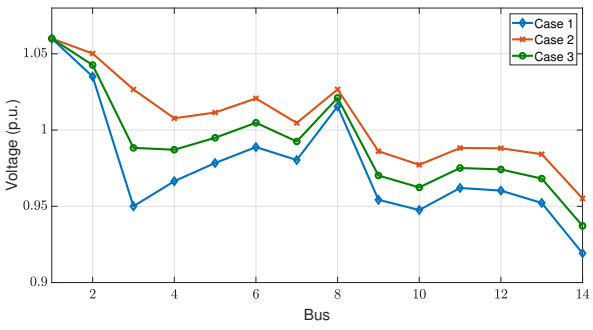

Fig. 3: IEEE 14 bus system node voltage magnitude comparison.

Fig 7 shows the bus 2 voltage of 14 bus system for a range of 0.9 to 1.9 loading factor. It can be seen that the bus voltage values are largely varying especially for case 1 and case 2, the lowest being at a loading factor 1.4. For case 3, both objectives from case 1 and 2 is incorporated so the voltage profile is much more stable. Similar trend is seen for the cost comparison case. The cost profiles from case 1 and case 2 are shown in Fig 8. It is evident that, to maximize the system stability the cost has been increased than the total cost in case

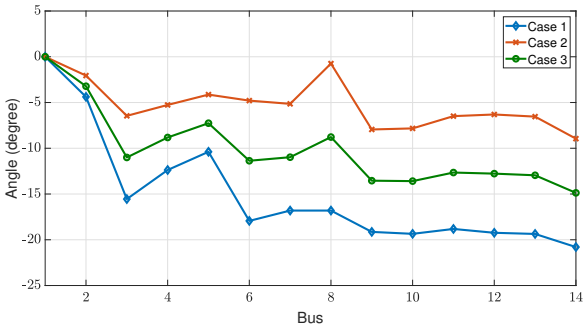

Fig. 4: IEEE 14 bus system node voltage angle comparison.

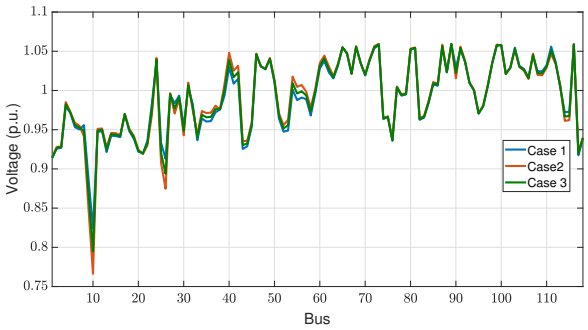

Fig. 5: IEEE 118 bus system node voltage magnitude comparison.

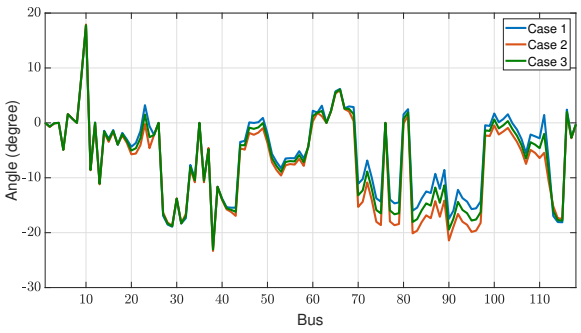

Fig. 6: IEEE 118 bus system node voltage angle comparison.

1. To prove the scalability of the algorithm, similar figures are represented in Fig 9 and Fig 10 for IEEE 118 bus system. From Fig 11 and 12, the minimum bus voltage of each test system has been compared, where the previous trend for the node voltage change in case 3 is justified. It can be seen that the minimum voltage occurs at loading factors 1.5 - 1.8.

In Table II and III total active power generation for all 3 cases, total connected loads and line losses are shown. Table V shows the comparison of total generation cost. From these comparison it is evident that, case 1 provides the solution for minimum cost, case 2 provides maximum stability margin with a notably higher cost, but in case 3 for a rise in cost the solution ensures maximum stability margin.

In Fig 13, the voltage magnitude profiles (critical voltage, with case 1, case 2 and case 3) of bus 2 for different loading factors are shown. It can be seen from the figure that, the voltage profile of case 2 is most stable compare to the profile in case 1. For case 3, the voltage profile is better than in case

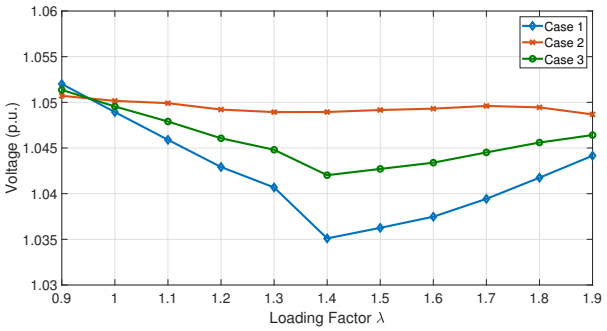

Fig. 7: IEEE 14 bus system bus 2 node voltage comparison.

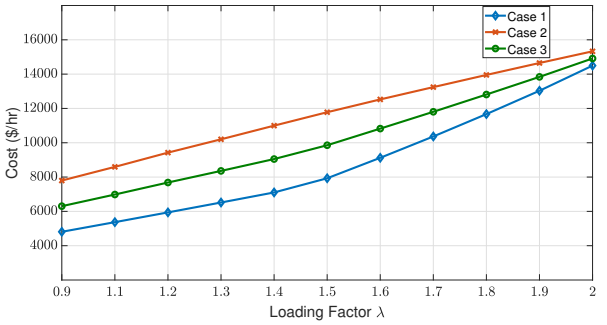

Fig. 8: IEEE 14 bus system total generation cost comparison for bus 2.

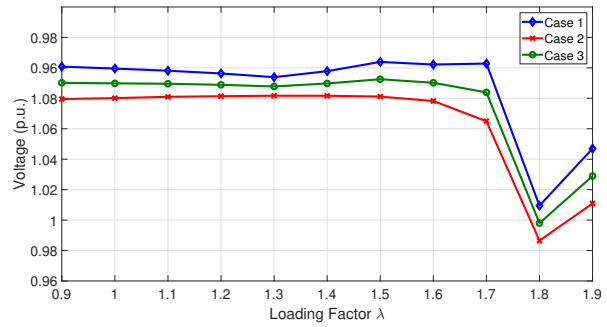

Fig. 9: IEEE 118 bus system node voltage comparison for bus 10.

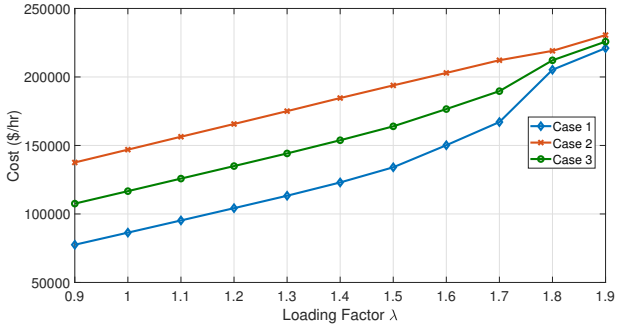

Fig. 10: IEEE 118 bus system total generation cost comparison for bus 10.

1. Also, Table V represents the distance to collapse for various loading factors for each case. For case 1, the system voltage is very close to the critical voltage value while in case 3, the distance is notably improved.

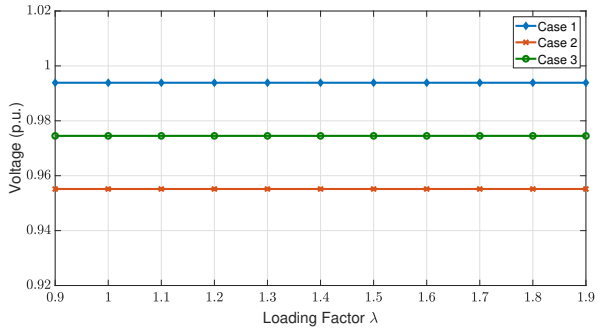

Fig. 11: IEEE 14 bus system minimum voltage comparison.

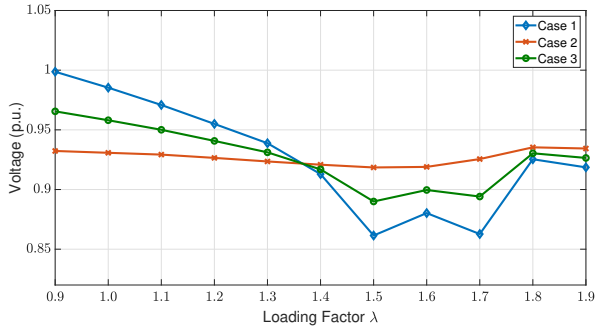

Fig. 12: IEEE 118 bus system minimum voltage comparison

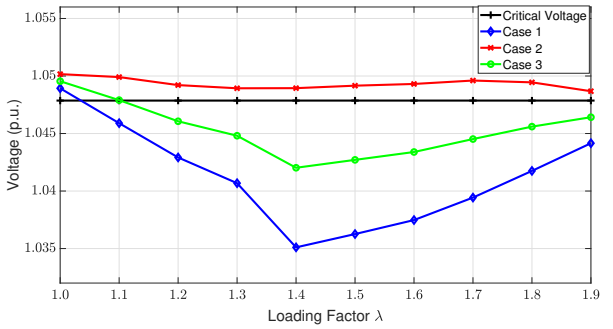

Fig. 13: Comparison of the operating voltage with the critical voltage of IEEE 14 Bus System

V. Conclusions and Future Work

Previous studies for optimal power flow in power system networks either emphasizes on cost or line loss minimizing

TABLE I: Generator cost coefficients in IEEE 14 Bus System

Gen	Bus	Cost ($/MW)
1	Bus 1	20
2	Bus 2	20
3	Bus 3	40
4	Bus 6	40
5	Bus 8	40

TABLE II: Comparison of power generation, total load and active power loss for IEEE 14 Bus System

	Case1	Case2	Case3
P_g(MW)	268.5744	287.9147	278.446
P_d(MW)	259	259	259
P_{loss}(MW)	9.5744	28.9147	19.2446

TABLE III: Comparison of power generation, total load and active power loss for IEEE 118 Bus System

	Case1	Case2	Case3
P_g(MW)	4318.428	5271.601	4795.014
P_d(MW)	4242	4242	4242
P_{loss}(MW)	76.427	1029.601	553.014

TABLE IV: Power generation cost comparison for IEEE 14 Bus and 118 Bus System

	Case1	Case2	Case3
14 Bus($/hr)	5371.487	8593.777	6982.632
118 Bus($/hr)	86366.43	146938.9	116652.7

TABLE V: Difference of critical voltage and operating voltage

Loading factor, (λ)	Case1 $\lvert V_1 - V_c \rvert$ [p.u.]	Case2 $\lvert V_2 - V_c \rvert$ [p.u.]	Case3 $\lvert V_3 - V_c \rvert$ [p.u.]
1.0	0.001068	0.002299	0.002005
1.1	0.001965	0.002043	0.003512
1.2	0.004944	0.001347	0.005229
1.3	0.007181	0.001070	0.006471
1.4	0.012761	0.001080	0.009180
1.5	0.011604	0.001295	0.008669
1.6	0.010387	0.001445	0.007957
1.7	0.008432	0.001742	0.006329
1.8	0.006113	0.001584	0.004007
1.9	0.003708	0.000815	0.001489

or system stability maximizing. In those approaches the other objective has been neglected. In this paper, both the stability and cost objectives are utilized to achieve a solution that ensures a more stable power system operating at a significantly lower cost. The combination of both cost minimization and stability margin maximization with weighting factors in the objective function, makes the total problem a non-linear convex optimization. This type of problem is not feasible for the common solvers such as MOSEK, to solve. In future, further studies will be conducted to convexify the whole problem applying proper relaxations.

REFERENCES

[1] J. D. Mountford, "Practical applications of optimal power flow," in *IEE Colloquium on Optimal Power Flow - Invaluable Tool or Expensive Toy? (Digest No: 1997/102)*, May 1997, pp. 3/1–3/7.

[2] M. Huneault and F. D. Galiana, "A survey of the optimal power flow literature," *IEEE Transactions on Power Systems*, vol. 6, no. 2, pp. 762–770, May 1991.

[3] Y. Shi, H. D. Tuan, S. W. Su, and H. H. M. Tam, "Nonsmooth optimization for optimal power flow over transmission networks," in *2015 IEEE Global Conference on Signal and Information Processing (GlobalSIP)*, Dec 2015, pp. 1141–1144.

[4] Zhifeng Qiu, G. Deconinck, and R. Belmans, "A literature survey of optimal power flow problems in the electricity market context," in *2009 IEEE/PES Power Systems Conference and Exposition*, March 2009, pp. 1–6.

[5] S. Punitha and K. Sundararaju, "Voltage stability improvement in power system using optimal power flow with constraints," in *2017 IEEE International Conference on Electrical, Instrumentation and Communication Engineering (ICEICE)*, April 2017, pp. 1–6.

[6] T. Zabaiou and L. Dessaint, "Vsc-opf based on line voltage indices for power system losses minimization and voltage stability improvement," in *2013 IEEE Power Energy Society General Meeting*, July 2013, pp. 1–5.

[7] G. G. Lage, G. R. M. da Costa, and C. A. Cañizares, "Limitations of assigning general critical values to voltage stability indices in voltage-stability-constrained optimal power flows," in *2012 IEEE International Conference on Power System Technology (POWERCON)*, Oct 2012, pp. 1–6.

[8] D. K. Molzahn, F. Dörfler, H. Sandberg, S. H. Low, S. Chakrabarti, R. Baldick, and J. Lavaei, "A survey of distributed optimization and control algorithms for electric power systems," *IEEE Transactions on Smart Grid*, vol. 8, no. 6, pp. 2941–2962, Nov 2017.

[9] A. Venzke, L. Halilbasic, U. Markovic, G. Hug, and S. Chatzivasileiadis, "Convex relaxations of chance constrained ac optimal power flow," in *2018 IEEE Power Energy Society General Meeting (PESGM)*, Aug 2018, pp. 1–1.

[10] R. Madani, J. Lavaei, and R. Baldick, "Convexification of power flow equations in the presence of noisy measurements," *IEEE Transactions on Automatic Control*, pp. 1–1, 2019.

[11] M. Ashraphijuo, S. Fattahi, J. Lavaei, and A. Atamtürk, "A strong semidefinite programming relaxation of the unit commitment problem," in *2016 IEEE 55th Conference on Decision and Control (CDC)*, Dec 2016, pp. 694–701.

[12] S. H. Low, "Convex relaxation of optimal power flow—part i: Formulations and equivalence," *IEEE Transactions on Control of Network Systems*, vol. 1, no. 1, pp. 15–27, March 2014.

[13] S. Moghadasi and S. Kamalasadan, "Real-time optimal scheduling of smart power distribution systems using integrated receding horizon control and convex conic programming," in *2014 IEEE Industry Application Society Annual Meeting*, Oct 2014, pp. 1–7.

[14] J. Lavaei and S. H. Low, "Zero duality gap in optimal power flow problem," *IEEE Transactions on Power Systems*, vol. 27, no. 1, pp. 92–107, Feb 2012.

[15] S. Moghadasi and S. Kamalasadan, "Optimal fast control and scheduling of power distribution system using integrated receding horizon control and convex conic programming," *IEEE Transactions on Industry Applications*, vol. 52, no. 3, pp. 2596–2606, May 2016.

[16] M. Khanabadi, S. Moghadasi, and S. Kamalasadan, "Real-time optimization of distribution system considering interaction between markets," in *2013 IEEE Industry Applications Society Annual Meeting*, Oct 2013, pp. 1–8.

[17] S. Moghadasi and S. Kamalasadan, "An architecture for voltage stability constrained optimal power flow using convex semi-definite programming," in *2015 North American Power Symposium (NAPS)*, Oct 2015, pp. 1–6.

[18] R. Madani, S. Sojoudi, and J. Lavaei, "Convex relaxation for optimal power flow problem: Mesh networks," *IEEE Transactions on Power Systems*, vol. 30, no. 1, pp. 199–211, Jan 2015.

[19] S. Moghadasi and S. Kamalasadan, "Voltage security cost assessment of integrated ac-dc systems using semidefinite programming," in *2016 IEEE Power Energy Society Innovative Smart Grid Technologies Conference (ISGT)*, Sep. 2016, pp. 1–5.

[20] W. Rosehart, C. Canizares, and V. Quintana, "Costs of voltage security in electricity markets," in *2000 Power Engineering Society Summer Meeting (Cat. No.00CH37134)*, vol. 4, July 2000, pp. 2115–2120 vol. 4.